

CONF-960765-57

RECEIVED

JUN 09 1997

OSTI SLAC-PUB-7228
July 1996

Measurement of time-dependent $B_d^0 - \bar{B}_d^0$ mixing using inclusive semileptonic decays**

The SLD Collaboration*
Stanford Linear Accelerator Center
Stanford University, Stanford, CA 94309

Abstract

The time dependence of $B_d^0 - \bar{B}_d^0$ mixing has been observed in events containing high- P_t leptons using a highly inclusive vertexing method to determine the B decay position. The initial state B hadron flavor was determined using the large forward-backward asymmetry provided by the highly polarized electron beam of SLC in combination with a jet charge technique. From a sample of 150,000 hadronic Z^0 decays observed in the SLD detector at the SLC between 1993 and 1995, a preliminary analysis of the mass difference between the two B_d^0 mass eigenstates yields $\Delta m_d = 0.520 \pm 0.072(\text{stat}) \pm 0.035(\text{syst}) \text{ ps}^{-1}$.

Contributed to the XXVIII International Conference on High Energy Physics,
Warsaw, Poland, July 25-31, 1996

MASTER

**This work was supported by Department of Energy contracts: DE-FG02-91ER40676 (BU), DE-FG03-92ER40701 (CIT), DE-FG03-91ER40618 (UCSB), DE-FG03-92ER40689 (UCSC), DE-FG03-93ER40788 (CSU), DE-FG02-91ER40672 (Colorado), DE-FG02-91ER40677 (Illinois), DE-AC03-76SF00098 (LBL), DE-FG02-92ER40715 (Massachusetts), DE-AC02-76ER03069 (MIT), DE-FG06-85ER40224 (Oregon), DE-AC03-76SF00515 (SLAC), DE-FG05-91ER40627 (Tennessee), DE-AC02-76ER00881 (Wisconsin), DE-FG02-92ER40704 (Yale); National Science Foundation grants: PHY-91-13428 (UCSC), PHY-89-21320 (Columbia), PHY-92-04239 (Cincinnati), PHY-88-17930 (Rutgers), PHY-88-19316 (Vanderbilt), PHY-92-03212 (Washington); the UK Science and Engineering Research Council (Brunel and RAL); the Istituto Nazionale di Fisica Nucleare of Italy (Bologna, Ferrara, Frascati, Pisa, Padova, Perugia); and the Japan-US Cooperative Research Project on High Energy Physics (Nagoya, Tohoku).

DISCLAIMER

This report was prepared as an account of work sponsored by an agency of the United States Government. Neither the United States Government nor any agency thereof, nor any of their employees, make any warranty, express or implied, or assumes any legal liability or responsibility for the accuracy, completeness, or usefulness of any information, apparatus, product, or process disclosed, or represents that its use would not infringe privately owned rights. Reference herein to any specific commercial product, process, or service by trade name, trademark, manufacturer, or otherwise does not necessarily constitute or imply its endorsement, recommendation, or favoring by the United States Government or any agency thereof. The views and opinions of authors expressed herein do not necessarily state or reflect those of the United States Government or any agency thereof.

DISCLAIMER

**Portions of this document may be illegible
in electronic image products. Images are
produced from the best available original
document.**

I Introduction

Particle-antiparticle mixing is a quantum mechanical effect that can occur in neutral meson systems where the flavor eigenstates and the mass eigenstates differ. In the case of the neutral B meson systems, the flavor eigenstates B° and \bar{B}° are related to the mass eigenstates, B_1 and B_2 , by

$$B^\circ = \frac{B_1 + B_2}{\sqrt{2}}$$

and

$$\bar{B}^\circ = \frac{B_1 - B_2}{\sqrt{2}}.$$

If the width difference in the mass eigenstates, $\Delta\Gamma$, is neglected, the probability that a given B° meson remains a B° meson at time t is given by

$$P(B^\circ \rightarrow B^\circ) = \frac{\Gamma}{2} e^{-\Gamma t} [1 + \cos \Delta m t],$$

and the probability that it oscillates into a \bar{B}° meson is

$$P(B^\circ \rightarrow \bar{B}^\circ) = \frac{\Gamma}{2} e^{-\Gamma t} [1 - \cos \Delta m t].$$

In these expressions, Δm is the absolute value of the mass difference between the two mass eigenstates. The time integrated probability that a B° mix into a \bar{B}° is given by

$$x = \frac{1}{2} \left[\frac{(\frac{\Delta m}{\Gamma})^2}{1 + (\frac{\Delta m}{\Gamma})^2} \right].$$

This is completely analogous to what has been studied in great detail in the neutral kaon system[1]. Time integrated mixing in the B meson system was first observed in hadron collisions[2]. The existing measurements at $\Upsilon(4s)$ give an average value of $\Delta m/\Gamma = 0.69 \pm 0.10$ [3]. The LEP experiments have recently measured time dependent $B_d^\circ - \bar{B}_d^\circ$ mixing using a number of different techniques[4]. In each of these measurements the flavor of the B hadron decaying on one side of the event is correlated with the flavor of the B hadron on the other side of the event to provide the mixing information. The flavor information is derived from the charge of high- P_t leptons, jet charge or reconstructed D^* charge. CDF has also observed time dependent mixing in proton-antiproton collisions using the correlation between lepton charges in high- P_t dilepton events[5]. These time dependent measurements yield a world average of $\Delta m_d = 0.457 \pm 0.019 \text{ ps}^{-1}$ [4].

In this paper, results are presented on a measurement of time-dependent $B_d^\circ - \bar{B}_d^\circ$ oscillations observed using data taken at the Stanford Linear Collider (SLC) with the Stanford Large Detector (SLD). The combination of the small spotsize and polarized electron beam of SLC and the superb vertex detector of SLD are well-suited

for measuring the time evolution of B mixing. In the analysis presented here 2609 events containing high- P_t leptons were selected from a sample of $\sim 150,000$ Z^0 decays recorded between 1993 and 1995. The data sample from 1993 consists of 50,000 Z^0 decays with an average electron beam longitudinal polarization of $63.0 \pm 1.1\%$. The additional 100,000 events collected in 1994 and 1995 has an average polarization of $77.2 \pm 0.5\%$.

The technique used here to measure $B_d^0 - \bar{B}_d^0$ mixing includes a novel initial state tag. In addition to using flavor correlations between the two sides of a given event, via the opposite-side jet charge, the large forward-backward asymmetry provided by the highly polarized electron beam was used to tag the initial flavor of the B hadron. The final state was tagged by the charge of high- P_t leptons and a maximum likelihood fit to the mixed fraction as a function of proper time was used to extract Δm_d .

II The SLD Detector

This analysis utilized a subset of the SLD detector. Charged particle tracking was done using the central drift chamber (CDC) and the vertex detector (VXD)[6]. The CDC is 2m long and extends radially from 0.2m to 1.0m. It consists of 10 superlayers, providing efficient tracking coverage out to $|\cos(\theta)|=0.75$. An average spatial resolution of $70 \mu\text{m}$ was obtained with this device. The VXD consists of 9.2 cm long ladders of charged coupled devices (CCD's) placed on 4 concentric cylinders. The inner ladders are located 29 mm from the beam line and the outer ones at 41mm. On average, 2.3 CCD's are traversed by charged tracks originating from the interaction point. Charged tracks were reconstructed in the CDC and linked with pixel clusters in the VXD. A combined fit using the Billoir method[7] was performed. The angular errors of the CDC combined with local $\sigma(r\phi)$ and $\sigma(rz)$ of VXD clusters of $5 \mu\text{m}$ and $8 \mu\text{m}$, respectively, lead to an $r\phi$ (plane perpendicular to the e^+e^- beams) impact parameter resolution of $(\alpha, \beta)_{r\phi} = (13 \mu\text{m}, 70 \mu\text{m})$. The rz (plane containing the beam axis) impact parameter resolution is $(\alpha, \beta)_{rz} = (38 \mu\text{m}, 70 \mu\text{m})$ ¹.

The liquid argon calorimeter (LAC) was used in the event trigger and in the determination of event shape quantities, such as jet and thrust axes. The LAC[8] covers $98\% \pi \text{ sr}$. The radiator is Pb. It consists of a 21 radiation length thick electromagnetic (EM) section followed by a 2.8 interaction length hadronic (HAD) section. Each section is subdivided into two longitudinal layers. The tower segmentation is approximately 33 mrad in the EM section and 66 mrad in the HAD section. The electromagnetic energy resolution of the calorimeter is $\sim 15\%/\sqrt{E}$. The hadronic energy resolution is $\sim 60\%/\sqrt{E}$.

¹The impact parameter resolution function is parametrized as $\alpha \oplus \beta/P\sqrt{\sin^3\theta}$.

The warm iron calorimeter (WIC) was used for muon identification[9]. This device is constructed from four interaction lengths of 2 inch thick steel plates interleaved with sixteen layers of plastic streamer tubes. The WIC surrounds the LAC and magnet coil of SLD. It provided hit resolutions of 0.4 cm and 2.0 cm in the azimuthal and axial directions, respectively.

III Interaction Point Determination

The SLC Interaction Point (IP) centroid position in the xy plane transverse to the beam axis was reconstructed with a measured precision of $\sigma_{IP} = (7 \pm 2)\mu\text{m}$ using tracks in sets of ~ 30 hadronic Z° decays. The z position of the Z° decay was determined on an event-by-event basis using the median z position of tracks at their point of closest approach to the IP in the xy plane. Monte Carlo studies show this quantity is known to a precision of $\sim 52\mu\text{m}$ [10].

IV Monte Carlo Simulation

Parts of the analyses described in this paper used simulated events created with the Lund JETSET 7.4 Z° event generator[11] and the GEANT 3.21 detector simulation package[12]. The b-quark fragmentation followed the Peterson *et al.* parametrization[13]. B mesons were generated with $\tau = 1.55$ ps and B baryons with $\tau = 1.10$ ps. B hadron decays were modelled according to the CLEO B decay model tuned to reproduce the semileptonic B decay lepton spectra and the inclusive charmed hadron spectra, as well as the track multiplicities measured at the T(4S) by ARGUS and CLEO[14]. B baryon and charmed hadron decays were modelled using JETSET with, in the latter case, branching fractions tuned to ARGUS, CLEO and Mark III data[14].

V Event Selection

The SLD trigger was based on loose calorimetric criteria to eliminate primary beam related backgrounds such as conventional e^\pm and γ scattered from the beam pipe and masks and upstream beam-induced muons (unique to SLC). The former were reduced by total energy and asymmetry cuts, while the latter were reduced by utilizing the fine grained tower structure of the LAC and the pattern of energy deposition of the muons. Approximately 150,000 Z° decays were recorded by SLD during the runs used for this analysis.

Hadronic Z^0 events were selected off-line for analysis. For this analysis, the total energy from charged tracks was required to be >18 GeV. The thrust axis was required to lie well within the acceptance of the VXD ($|\cos(\theta)| < 0.71$). A minimum of seven reconstructed charged tracks was required in the drift chamber (to reduce $\gamma\gamma$ and $\tau\bar{\tau}$ backgrounds). Finally, to insure optimal CDC and VXD operation, known bad running periods were rejected and at least 3 tracks were required to have VXD links.

VI Track Selection

CDC tracks were required to start at a radius, $r \leq 40$ cm, have >40 hits, extrapolate to the IP within 1 cm in xy and 1.5 cm in z, and have good fit quality ($\chi^2/\text{d.o.f.} < 5$). At least one good VXD link was required and the combined CDC/VXD fit satisfied $\chi^2/\text{d.o.f.} < 5$. In addition, tracks having a 2-d impact parameter error greater than $250 \mu\text{m}$ and tracks with a 2-d impact parameter greater than 3 mm were removed. The former removed poorly measured tracks and the latter helped remove tracks from long-lived decays, i.e., strange particle decays and gamma conversions. Tracks that passed these cuts were considered to be of high quality and were used in the analysis.

VII B Selection

Events used in this analysis were selected by making use of the kinematic properties of semileptonic decays of B hadrons. Electron candidates were required to have energy deposits in the LAC which agreed with the momentum of tracks extrapolated from the CDC, to have little or no LAC hadronic energy and to have a front/back electromagnetic energy ratio consistent with that expected for electrons[15]. Electron candidates consistent with having come from a gamma conversion were removed from the sample. Muon candidates were required to have a good match between hits found in the WIC and tracks extrapolated from the CDC, taking into account track extrapolation errors and multiple scattering[15]. The sample was enriched in events containing B hadron decays by requiring that the lepton candidate have a momentum transverse to the nearest jet, $P_t > 0.8$ GeV/c, where jets were found using charged tracks with the JADE algorithm[16] with $y_{\text{cut}} = 0.015$.

A total of 5200 event hemispheres contain leptons passing the cuts described above. In instances where more than one lepton in a hemisphere passed the cuts, the lepton candidate with the highest value of

$$S = P_t^2 + \left(\frac{P}{15}\right)^2$$

was assumed to come from the B decay. Figure 1 shows the P_t distribution of the selected leptons for both the Monte Carlo and the data.

VIII B decay proper time determination

VIII.A Decay length estimate

The determination of an accurate proper time for each B hadron decay was essential to observe the time evolution of mixing. There were three important elements in the calculation of the proper time. They were the spatial position of the interaction point, the spatial position of the B decay and the relativistic boost of the decaying B hadron.

The B hadron decay length in the laboratory was determined from the difference between the positions of the interaction point and the B decay. The determination of the spatial position of the interaction point is described above in section III. The B hadron decay position was estimated as the weighted average position on the lepton track of the points of closest approach of all the quality charged tracks in the hemisphere containing the high- P_t lepton. Figure 2 provides a useful illustration of the method. This technique takes advantage of the fact that, after the P_t cut, the lepton is most likely from the B decay vertex, i.e., it should pass close to the B decay position. Intersecting this track with other tracks from the B or cascade charm decays should provide a reasonable determination of the B decay position. The weights are adjusted to lessen the contribution to the weighted average from tracks emanating from the interaction point or long-lived cascade charm decays. By taking the average over many tracks (~ 4 on average) the resolution on the B decay position is improved. More specifically, the vector from the interaction point to the B decay vertex, $\vec{X}_{B_{vtx}}$, is found by

$$\vec{X}_{B_{vtx}} = \frac{\sum W_i \vec{X}_i}{\sum W_i},$$

where \vec{X}_i is the vector from the interaction point to the point on the lepton track that is closest to the path of track i . W_i is the product of three weights, W_1 , W_2 and W_3 .

W_1 is given by

$$W_1 = \frac{x}{x + A} (1 - e^{(-x^2)}),$$

where $x = \sigma_3/B$ and $A=0.5$ and $B=4$ are constants determined by Monte Carlo studies. σ_3 is the normalized three dimensional impact parameter of the track. This function is designed to give more significance to tracks that are from secondary vertices. It takes advantage of the fact that tracks from the B and cascade charm decays

are more likely to have a large three dimensional normalized impact parameter. It approaches zero at small impact parameters and becomes approximately constant at very large impact parameter.

W_2 characterizes how well the intersection between the given track and the lepton is determined.

$$W_2 = \frac{\sin \theta}{\delta r},$$

where θ is the opening angle between the given track and the lepton and δr is the width of the track error ellipse as projected onto the lepton track.

W_3 gives more significance to tracks that intersect the lepton relatively close to where the jet axis intersects the lepton. It is given by

$$W_3 = e^{-\frac{\alpha}{C}},$$

where α is the opening angle between the jet axis and the vector from the interaction point to the point on the lepton closest to the given track. $C=2.5$ is a constant determined from Monte Carlo studies. This component to the weight is desirable because Monte Carlo studies show that the jet direction is very close to the B hadron direction.

Figure 3(a) shows the reconstructed B hadron decay length distribution in the laboratory determined using the method described above for both data and Monte Carlo. Note that the backgrounds from non-B events is concentrated at small decay lengths. This background was removed by requiring that the decay length be greater than $200 \mu\text{m}$ and that the reconstructed proper time of the event (described below) be greater than 0.25 ps , leaving 2997 lepton candidates in the analysis. An additional cut requiring the 3d normalized impact parameter of the lepton to the interaction point to be greater than 2.5 was also used to improve the B purity, leaving 2609 leptons for the mixing analysis.

Figure 3(b) shows the decay length residual for Monte Carlo events passing the cuts described above. This curve is well-described by two gaussians of widths $170 \mu\text{m}$ and $550 \mu\text{m}$, respectively, where the core gaussian constitutes 58% of the sample.

VIII.B Boost estimate

The relativistic boost of the B hadron was estimated by assuming energy and momentum conservation to determine the total energy of the jet containing the lepton (including any missing energy). Within the jet containing the lepton, the missing energy and that due to fragmentation tracks was estimated using kinematic and impact parameter information. The energy of the B hadron was given by subtracting the fragmentation energy from the total jet energy.

In more detail, the jets were found using charged tracks with $Y_c=0.015$. It was assumed that the number of initial partons and their directions were given by the number and directions of jets. Constraints due to momentum and energy conservation along with the determined jet directions were sufficient to estimate the total energy of the jet containing the high- P_t lepton. For two-jet events, the missing energy in the jet, E_ν , was taken to be the difference between the total energy of the jet and the visible energy of the jet, found summing all the visible charged and neutral energy in the hemisphere containing the jet. For three-jet events the visible energy in a cone about the jet axis was used to avoid double-counting energy. The cone was defined by using an opening angle equal to the maximum opening angle of an associated charged track with the jet axis. Four-jet events were handled in a similar fashion. In cases with more than four jets, the four highest energy jets were used.

The fraction of visible neutral energy in the whole jet that comes from the B decay was estimated on an event-by-event basis using a parametrization determined from Monte Carlo studies. More explicitly,

$$E_B^\circ = K_1 E^\circ + K_2 (E^\circ)^2,$$

where E° is the total visible neutral energy in the jet and E_B° is that visible neutral energy in the jet that is associated with the decay of the B hadron. The assumption in first term of this parametrization is that the ratio of the total energy of the B hadron to that in the jet is similar to the ratio of the total visible neutral energy of the B hadron to that in the jet. The second term adds a handle for fine-tuning the resolution. The constants 'K₁' and 'K₂' were set to 0.7 and 0.01, respectively.

The absolute value of the normalized three-dimensional impact parameter of tracks to the interaction point, σ_3 , was used to distinguish between charged tracks from fragmentation and those from the B decay. Charged tracks, excluding the lepton, that passed the standard quality cuts were ordered by descending σ_3 and divided into three categories. The categories were as follows: (I) secondary tracks, $\sigma_3 > 3.5$, (II) ambiguous tracks, $1 \leq \sigma_3 \leq 3.5$, and (III) primary tracks $\sigma_3 < 1$. The tracks in category (I) were combined together, in descending order, until the invariant mass of the combination, M_{inv} , was greater than $2.0 \text{ GeV}/c^2$. If $M_{inv} < 2.0 \text{ GeV}/c^2$ after using all the tracks in category (I), tracks in category (II) were used (again in descending order). If, after using all the tracks in categories (I) and (II), M_{inv} was less than $0.5 \text{ GeV}/c^2$, tracks from category (III) were added in until $M_{inv} > 0.5 \text{ GeV}/c^2$. In the end, the sum of the energies of tracks contributing to the invariant mass described above and the lepton was taken to be the visible charged energy of the decaying B hadron, E_B^\pm . All of the tracks were considered to be pions unless they were well-identified electrons or muons. The other charged tracks in the jet were considered to come from fragmentation processes.

The total energy of the decaying B hadron was taken to be equal to the sum of E_B^\pm , E_B° and E_ν . Figure 4 shows the reconstructed B hadron momentum distribution

in the laboratory determined using the relativistic boost described above for both data and Monte Carlo. Figure 5(a) and (b) show the boost residual and relative residual, respectively, for Monte Carlo events. This curve is well-described by two gaussians of widths 7.9% and 25%, respectively, where the core gaussian constitutes 50% of the sample. Events in these figures have passed the decay length ($>200 \mu\text{m}$) and proper time ($>0.25 \text{ ps}$) cuts.

The B hadron decay proper time, t , was determined from the decay length, X_{dl} , and the relativistic boost, $\beta\gamma$, as follows:

$$t = \frac{X_{dl}}{\beta\gamma} = \frac{m_B}{\sqrt{E_B^2 - M_b^2}} X_{dl}$$

Figure 6 (a) and (b) show the proper time residual and relative residual for Monte Carlo events passing the decay length and proper time cuts. Note that most of the events have a reconstructed proper time within 0.5 ps of the true proper time and that the tails are symmetric. Figure 7 shows the proper time distribution for all events that survived the cuts.

IX Mixing Analysis

IX.A Method

The probability of a given event being mixed was calculated using the charge of the lepton for the final state tag and the electron beam polarization and decaying hadron direction along with the opposite-side jet charge for the initial state tag. If the probability of mixing was greater than 50%, the event was categorized as 'mixed'. Otherwise the event was considered to be 'unmixed'. A maximum likelihood analysis was performed on the fraction of mixed events as a function of proper time with Δm_d as the free parameter.

IX.B Flavor tagging

Parity violation in the Z-fermion pair vertex leads to a well-understood forward backward asymmetry in Z° decays. The size of this asymmetry can be enhanced with the use of polarized electrons. The forward-backward asymmetry formed using polarization information has been measured for some fermions and is called the left-right forward-backward asymmetry[17], defined by

$$\tilde{A}_{LRFB}^f = \frac{[\sigma_L^f(z) - \sigma_L^f(-z)] - [\sigma_R^f(z) - \sigma_R^f(-z)]}{[\sigma_L^f(z) - \sigma_L^f(-z)] + [\sigma_R^f(z) - \sigma_R^f(-z)]}$$

$$\tilde{A}_{LRFB}^f = |P_e| A_f \frac{2z}{(1+z^2)}$$

where f is the fermion type in the final state, $z = \cos \theta$ is the direction of the outgoing fermion relative to the incident electron. The parameter $A_f = 2v_f a_f / (v_f^2 + a_f^2)$ expresses the extent of the parity violation in the Zff vertex in terms of the vector and axial vector coupling constant of the Z^0 to fermions. P_e is the longitudinal polarization of the electron beam. $P_e > 0 (< 0)$ for right-handed (left-handed) polarization, which is denoted by the subscript R(L). For the $Zb\bar{b}$ vertex the left-right forward-backward asymmetry is measured to be relatively large ($A_b \sim 0.9$)[17].

For a given event, the initial state flavor tagging probability found using the polarization tag was taken to be

$$G_{pol} = \frac{(1 + P_e A_e)(1 + z^2) + 2A_b(P_e + A_e)z}{2(1 + P_e A_e)(1 + z^2)}.$$

Further information concerning the production flavor of the b quark was obtained using the jet charge calculated in the hemisphere opposite the jet containing the high- P_t lepton. The jet charge was defined as

$$Q_H = \sum q_i |\vec{p}_i \cdot \vec{T}|^\kappa,$$

where the sum is over tracks in the hemisphere, q_i is the charge of the i^{th} track, \vec{p}_i is its momentum, \vec{T} is the thrust axis and κ is a constant set to be 0.5. For a given event, the flavor tagging probability using the jet charge tag was given by

$$G_{jc} = \frac{1}{1 + e^{\alpha Q_H}}.$$

α quantifies the jet charge analyzing power and was determined by Monte Carlo studies to be 0.32. Combining this with the information from the polarization tag yields the total initial state flavor tagging probability for a specific event,

$$G = \frac{G_{jc} G_{pol}}{G_{jc} G_{pol} + (1 - G_{jc})(1 - G_{pol})}.$$

The combined correct tag probability for the initial state was determined from Monte Carlo events to be 80%.

The final state flavor tag was determined by the sign of the charge of the high- P_t lepton. The correct tag probability for the final state was determined to be 85% by a Monte Carlo study.

The probability of mixing, that is to say, the probability that a B hadron vertex produced by a decaying $b(\bar{b})$ quark originated as a particle carrying a $\bar{b}(b)$ quark, was given by

$$P_M = P_i(b)P_f(\bar{b}) + P_i(\bar{b})P_f(b).$$

Events containing high- P_t leptons were tagged as 'mixed' if $P_M > 0.5$. Otherwise they were tagged as 'unmixed'.

IX.C Likelihood function

In order to construct the likelihood function, L , probability density functions, P_i^{mixed} and $P_i^{unmixed}$, for leptons tagged as mixed and unmixed, respectively, were parametrized. The likelihood function is given by

$$L = \prod_{i,unmixed} [G \cdot P_i^{unmixed} + (1 - G) \cdot P_i^{mixed}] \prod_{j,mixed} [G \cdot P_j^{mixed} + (1 - G) \cdot P_j^{unmixed}]$$

The functions, P_i^{mixed} and $P_i^{unmixed}$, represent the time evolved probability densities of the mixed and unmixed events, taking into account all the possible origins of the leptons and the proper time resolution of the detector.

Ignoring the proper time resolution of the detector, the time evolution of the unmixed and mixed states was given by

$$\begin{aligned} F(t)_{unmixed} = & f_{B_d^0 \rightarrow (l^\pm, X^\pm)} \frac{e^{-t/\tau_{B_d^0}}}{\tau_{B_d^0}} \frac{1}{2} \left(1 + \cos x_d \frac{t}{\tau_{B_d^0}} \right) \\ & + f_{B_s^0 \rightarrow (l^\pm, X^\pm)} \frac{e^{-t/\tau_{B_s^0}}}{\tau_{B_s^0}} \frac{1}{2} \left(1 + \cos x_s \frac{t}{\tau_{B_s^0}} \right) + f_{B^\pm \rightarrow (l^\pm, X^\pm)} \frac{e^{-t/\tau_{B^\pm}}}{\tau_{B^\pm}} \\ & + f_{\bar{c}c} (1 - \lambda) \frac{e^{-t/\tau_c}}{\tau_c} + f_{\Lambda_b \rightarrow (l^\pm, X^\pm)} \frac{e^{-t/\tau_{\Lambda_b}}}{\tau_{\Lambda_b}} + \frac{f_{uds}}{2} \frac{e^{-t/\tau_{uds}}}{\tau_{uds}} \\ & + \frac{f_{B_d^0 \rightarrow c \rightarrow (l^\pm, X^\pm)}}{2\tau_{B_d^0}} \int_0^t e^{-\frac{(t-t')}{\tau_{B_d^0}}} \left(1 - \cos x_d \frac{t-t'}{\tau_{B_d^0}} \right) e^{-\frac{t'}{\tau_c}} \frac{dt'}{\tau_c} \\ & + \frac{f_{B_s^0 \rightarrow c \rightarrow (l^\pm, X^\pm)}}{2\tau_{B_s^0}} \int_0^t e^{-\frac{(t-t')}{\tau_{B_s^0}}} \left(1 - \cos x_s \frac{t-t'}{\tau_{B_s^0}} \right) e^{-\frac{t'}{\tau_c}} \frac{dt'}{\tau_c} \\ & + \frac{f_{B^\pm \rightarrow c \rightarrow (l^\pm, X^\pm)}}{2\tau_{B^\pm}} \int_0^t e^{-\frac{(t-t')}{\tau_{B^\pm}}} e^{-\frac{t'}{\tau_c}} \frac{dt'}{\tau_c} \\ & + \frac{f_{\Lambda_b \rightarrow c \rightarrow (l^\pm, X^\pm)}}{2\tau_{\Lambda_b}} \int_0^t e^{-\frac{(t-t')}{\tau_{\Lambda_b}}} e^{-\frac{t'}{\tau_c}} \frac{dt'}{\tau_c} \end{aligned}$$

and

$$\begin{aligned} F(t)_{mixed} = & f_{B_d^0 \rightarrow (l^\pm, X^\pm)} \frac{e^{-t/\tau_{B_d^0}}}{\tau_{B_d^0}} \frac{1}{2} \left(1 - \cos x_d \frac{t}{\tau_{B_d^0}} \right) \\ & + f_{B_s^0 \rightarrow (l^\pm, X^\pm)} \frac{e^{-t/\tau_{B_s^0}}}{\tau_{B_s^0}} \frac{1}{2} \left(1 - \cos x_s \frac{t}{\tau_{B_s^0}} \right) + f_{B^\pm \rightarrow (l^\pm, X^\pm)} \frac{e^{-t/\tau_{B^\pm}}}{\tau_{B^\pm}} \\ & + f_{\bar{c}c} \lambda \frac{e^{-t/\tau_c}}{\tau_c} + f_{\Lambda_b \rightarrow (l^\pm, X^\pm)} \frac{e^{-t/\tau_{\Lambda_b}}}{\tau_{\Lambda_b}} + \frac{f_{uds}}{2} \frac{e^{-t/\tau_{uds}}}{\tau_{uds}} \\ & + \frac{f_{B_d^0 \rightarrow c \rightarrow (l^\pm, X^\pm)}}{2\tau_{B_d^0}} \int_0^t e^{-\frac{(t-t')}{\tau_{B_d^0}}} \left(1 + \cos x_d \frac{t-t'}{\tau_{B_d^0}} \right) e^{-\frac{t'}{\tau_c}} \frac{dt'}{\tau_c} \\ & + \frac{f_{B_s^0 \rightarrow c \rightarrow (l^\pm, X^\pm)}}{2\tau_{B_s^0}} \int_0^t e^{-\frac{(t-t')}{\tau_{B_s^0}}} \left(1 + \cos x_s \frac{t-t'}{\tau_{B_s^0}} \right) e^{-\frac{t'}{\tau_c}} \frac{dt'}{\tau_c} \end{aligned}$$

$$\begin{aligned}
& + \frac{f_{B_d^\pm \rightarrow c \rightarrow (l^\pm, X^\pm)}}{2\tau_{B_d^\pm}} \int_0^t e^{-\frac{(t-t')}{\tau_{B_d^\pm}}} e^{-\frac{t'}{\tau_c}} \frac{dt'}{\tau_c} \\
& + \frac{f_{\Lambda_b \rightarrow c \rightarrow (l^\pm, X^\pm)}}{2\tau_{\Lambda_b}} \int_0^t e^{-\frac{(t-t')}{\tau_{\Lambda_b}}} e^{-\frac{t'}{\tau_c}} \frac{dt'}{\tau_c}
\end{aligned}$$

Most of the notation is straightforward. For example, $\tau_{B_d^\pm}$ is the average lifetime of B_d^\pm mesons. $f_{B_d^\pm \rightarrow (l^\pm, X^\pm)}$ is the fraction of B_d^\pm mesons that decay into a final state containing a lepton (l^\pm) or a track that fakes a lepton (X^\pm) with the correct charge sign. $f_{c\bar{c}}$ is the fraction of leptons in the sample that come from $Z^0 \rightarrow c\bar{c}$ events. f_{uds} is fraction of leptons in the sample that come from $Z^0 \rightarrow u\bar{u}$, $d\bar{d}$ or $s\bar{s}$ (so-called uds events). τ_c and τ_{uds} are the average charmed hadron lifetime and the effective lifetime for leptons from uds events events, respectively. Finally, λ represents the fraction of charmed hadron decays into a lepton with the same charge as that of the c quark in the decaying hadron. The other variables are self-explanatory or previously defined.

The constrained parameters used in the maximum likelihood analysis are summarized in Table 1. For data, the constrained parameters were determined by experiment where possible and estimated by Monte Carlo studies when no experimental result was available. For the analysis of Monte Carlo events, the constrained parameters were fixed to the values used in the Monte Carlo.

The time evolved probability densities of the mixed and unmixed events were obtained by convoluting the functions, $F(t)_{mixed}$ and $F(t)_{unmixed}$, with the experimental proper time resolution function for the detector as determined by Monte Carlo studies.

$$P_i^{unmixed} = \int_0^\infty F(t_0)_{unmixed} [f_1 g_1(t_0, t) + (1 - f_1) g_2(t_0, t)] dt_0$$

and

$$P_i^{mixed} = \int_0^\infty F(t_0)_{mixed} [f_1 g_1(t_0, t) + (1 - f_1) g_2(t_0, t)] dt_0,$$

where g_1 and g_2 are gaussian functions with widths $\sigma_1 = 0.18$ ps and $\sigma_2 = 0.54$ ps, respectively. The relative fraction of the events in the core gaussian, f_1 , was taken to be 0.54%.

IX.D Results

Figure 8 shows the mixed fraction as a function of the proper time for data. Also shown are expected curves for the best fit and the case for no $B_d^\pm - \bar{B}_d^\pm$ mixing (x_s was taken to be 10). The maximum likelihood fit yields a value of $\Delta m_d = 0.520 \pm 0.072(\text{stat})$. The log likelihood curve is given in Figure 9 as a function of Δm_d .

As a check of the analysis procedure, a Monte Carlo sample of similar size was used as input in the analysis. The results are shown in Figures 10 and 11. The

Parameter	value
Δm_s	6.5
$f_{c\bar{c}}$	0.053
f_{uds}	0.02
λ	0.54
$f_{B_d^0 \rightarrow (l^\pm, X^\pm)}$	31.3% right-sign 0.8% wrong-sign
$f_{B_s^0 \rightarrow (l^\pm, X^\pm)}$	8.5% right-sign 0.15% wrong-sign
$f_{B^\pm \rightarrow (l^\pm, X^\pm)}$	32.65% right-sign 0.45% wrong-sign
$f_{\Lambda_b \rightarrow (l^\pm, X^\pm)}$	6.0% right-sign 0.15% wrong-sign
$f_{B_d^0 \rightarrow c \rightarrow (l^\pm, X^\pm)}$	2.0% right-sign 6.0% wrong-sign
$f_{B_s^0 \rightarrow c \rightarrow (l^\pm, X^\pm)}$	0.5% right-sign 1.35% wrong-sign
$f_{B^\pm \rightarrow c \rightarrow (l^\pm, X^\pm)}$	2.15% right-sign 5.8% wrong-sign
$f_{\Lambda_b \rightarrow c \rightarrow (l^\pm, X^\pm)}$	0.2% right-sign 0.5% wrong-sign
$\tau_{B_d^0}$	1.55 ps
$\tau_{B_s^0}$	1.55 ps
τ_{B^\pm}	1.55 ps
τ_{Λ_b}	1.10 ps
τ_c	0.5 ps
τ_{uds}	0.3 ps
A_b	0.94
α	0.32

Table 1: Constrained parameters used in the maximum likelihood analysis.

Monte Carlo input for Δm_d was 0.503 and the measured value was $\Delta m_d = 0.488 \pm 0.075(\text{Stat})$.

X Systematic Errors

The primary sources of systematic error in these measurements are listed in the first column of Table 2. For most of the quantities listed in the table, the effect of a variation on the measured value of Δm_d was determined by varying its value in the maximum likelihood function. The central value and 1σ variation for each quantity is listed in column two of Table 2. The third column of the table gives the 1σ variation induced in measured value of Δm_d from the variation of the quantities in the table.

Detailed checks of the track resolution modeling were performed. It was found that the simulation reproduces the distribution of the track impact parameters in the $r\phi$ plane very well, but appeared to be somewhat narrower than the data in the core of the impact parameter distribution in the rz plane. This is attributed to residual misalignments within the vertex detector. A correction was applied to account for this and the quoted systematic uncertainty corresponds to the difference between results obtained with and without this correction.

The error in Δm_d due to the boost determination was evaluated by multiplying the boost of events in the data by a constant such that the average boost in the data agreed with that in the Monte Carlo. The shift in Δm_d after this adjustment was taken as the systematic error.

XI Summary

From a sample of 150,000 Z^0 decays recorded with the SLD detector at the SLC during 1993-1995, the time dependence of $B_d^0 - \bar{B}_d^0$ mixing has been observed in events where a B hadron decays semileptonically. The B hadron decay position was reconstructed using an inclusive technique with a decay length resolution of $\sim 170 \mu m$ and an efficiency of $\sim 98\%$. The initial state flavor tag was accomplished using the forward-backward asymmetry, enhanced by the polarization of the electron beam, and the opposite-side jet charge. The final state flavor tag was given by the charge of the lepton. The time dependence $B_d^0 - \bar{B}_d^0$ mixing was observed by fitting the oscillation in the fraction of mixed events as a function of proper time. The preliminary analysis yields $\Delta m_d = 0.520 \pm 0.072(\text{stat}) \pm 0.035(\text{syst}) \text{ ps}^{-1}$.

quantity	nominal \pm range	$\delta \Delta m_d \text{ ps}^{-1}$
detector resolution	-	± 0.013
tracking efficiency	-	negl.
lepton ID efficiency	-	negl.
Boost	5.785 ± 0.041	± 0.008
B_d^0 lifetime	$1.55 \pm 0.10 \text{ ps}$	± 0.009
B_s^0 lifetime	$1.55 \pm 0.15 \text{ ps}$	± 0.001
B_{baryon} lifetime	$1.10 \pm 0.11 \text{ ps}$	± 0.004
τ_c parametrization	0.4 ± 0.05	± 0.005
B_s^0 fraction	$(11.5 \pm 3)\%$	± 0.014
B_{baryon} fraction	$(7.2 \pm 3)\%$	± 0.015
$\Delta m_s (\text{ps}^{-1})$	$6.5^{+\infty}_{-1.5}$	± 0.006
$f_{b \rightarrow c \rightarrow l}$	$(14 \pm 1)\%$	± 0.013
$\text{BR}(B_d^0 \rightarrow c \rightarrow l/b \rightarrow c \rightarrow l)$	$(6.5 \pm 1)\%$	± 0.006
Background parameters	f_{cc}, f_{uds}	± 0.0024
Tagging parameters	$P_e, \pm 1.0\%$ $A_b, \pm 4\%$ $\alpha, \pm 10\%$	± 0.014
Total systematic error		± 0.035

Table 2: Summary of systematic errors.

Acknowledgments We would like to thank the personnel of the SLAC accelerator department and the technical staffs of our collaborating institutions for their outstanding efforts on our behalf.

References

- [1] Review of particle properties, Phys Rev D50 (1994) 1173.
- [2] C. Albajar *et al.*, Phys. Lett. B186 (1987) 237, 247.
- [3] J.Bartel *et al.* (CLEO Collaboration), CLNS/93-1207 (1993),
H Albrecht *et al.* (ARGUS Collaboration), Z. Phys. C55 (1992).
- [4] Sau Lan Wu, *Recent Results on B Meson Oscillations*, WISC-EX-96-343, 1996;
presented at the XVII International Symposium on Lepton-Photon Interactions,
Beijing, China, August 1995.
- [5] CDF Collaboration, *Measurement of $B^0 - \bar{B}^0$ Mixing via Time Evolution*,
contributed to the XVII International Symposium on Lepton-Photon Interactions,
Beijing, China, August 1995.

- [6] G. Agnew *et al.*, SLAC-PUB-5906;
 Also in the Proceedings of the 26th International
 Conference on High Energy Physics, Dallas, Texas, USA, August 1992.
- [7] P. Billoir, Nucl. Inst. and Meth. **225**, 352 (1984).
- [8] D. Axen *et al.*, Nucl. Instr. and Meth. **A238**, 472 (1993).
- [9] A. Benvenuti *et al.*, Nucl. Inst. Meth. **A276**, 94 (1989); **A290**, 353 (1990).
- [10] K. Abe *et al.* (SLD Collaboration), Phys. Rev. **D53**, 1023 (1996).
- [11] T. Sjöstrand, CERN-TH-7112-93, Feb. 1994.
- [12] R. Brun, F. Bruyant, M. Maire, A.C. McPherson and P. Zanarini, CERN
 DD/EE/84-1, September 1987.
- [13] C. Peterson *et al.*, Phys. Rev. **D27**, 105 (1983).
- [14] T.R. Junk, Ph.D. Thesis, Stanford University, SLAC-Report-95-476, Nov. 1995.
- [15] K. Abe *et al.* (SLD Collaboration), Phys. Rev. Lett. **74**, 2895 (1995).
- [16] W. Bartel *et al.* (JADE Collaboration), Z. Phys. **C33**, 23 (1986).
- [17] K. Abe *et al.* (SLD Collaboration), Phys. Rev. Lett. **74** (1995), p. 2890 and
 2895.

*List of Authors

K. Abe,⁽¹⁹⁾ K. Abe,⁽²⁹⁾ I. Abt,⁽¹³⁾ T. Akagi,⁽²⁷⁾ N.J. Allen,⁽⁴⁾ W.W. Ash,^{(27)†}
 D. Aston,⁽²⁷⁾ K.G. Baird,⁽²⁴⁾ C. Baltay,⁽³³⁾ H.R. Band,⁽³²⁾ M.B. Barakat,⁽³³⁾
 G. Baranko,⁽⁹⁾ O. Bardon,⁽¹⁵⁾ T. Barklow,⁽²⁷⁾ A.O. Bazarko,⁽¹⁰⁾ R. Ben-David,⁽³³⁾
 A.C. Benvenuti,⁽²⁾ G.M. Bilei,⁽²²⁾ D. Bisello,⁽²¹⁾ G. Blaylock,⁽⁶⁾ J.R. Bogart,⁽²⁷⁾
 B. Bolen,⁽¹⁷⁾ T. Bolton,⁽¹⁰⁾ G.R. Bower,⁽²⁷⁾ J.E. Brau,⁽²⁰⁾ M. Breidenbach,⁽²⁷⁾
 W.M. Bugg,⁽²⁸⁾ D. Burke,⁽²⁷⁾ T.H. Burnett,⁽³¹⁾ P.N. Burrows,⁽¹⁵⁾ W. Busza,⁽¹⁵⁾
 A. Calcaterra,⁽¹²⁾ D.O. Caldwell,⁽⁵⁾ D. Calloway,⁽²⁷⁾ B. Camanzi,⁽¹¹⁾
 M. Carpinelli,⁽²³⁾ R. Cassell,⁽²⁷⁾ R. Castaldi,^{(23)(a)} A. Castro,⁽²¹⁾
 M. Cavalli-Sforza,⁽⁶⁾ A. Chou,⁽²⁷⁾ E. Church,⁽³¹⁾ H.O. Cohn,⁽²⁸⁾ J.A. Coller,⁽³⁾
 V. Cook,⁽³¹⁾ R. Cotton,⁽⁴⁾ R.F. Cowan,⁽¹⁵⁾ D.G. Coyne,⁽⁶⁾ G. Crawford,⁽²⁷⁾
 A. D’Oliveira,⁽⁷⁾ C.J.S. Damerell,⁽²⁵⁾ M. Daoudi,⁽²⁷⁾ R. De Sangro,⁽¹²⁾
 R. Dell’Orso,⁽²³⁾ P.J. Dervan,⁽⁴⁾ M. Dima,⁽⁸⁾ D.N. Dong,⁽¹⁵⁾ P.Y.C. Du,⁽²⁸⁾
 R. Dubois,⁽²⁷⁾ B.I. Eisenstein,⁽¹³⁾ R. Elia,⁽²⁷⁾ E. Etzion,⁽⁴⁾ D. Falciai,⁽²²⁾ C. Fan,⁽⁹⁾
 M.J. Fero,⁽¹⁵⁾ R. Frey,⁽²⁰⁾ K. Furuno,⁽²⁰⁾ T. Gillman,⁽²⁵⁾ G. Gladding,⁽¹³⁾
 S. Gonzalez,⁽¹⁵⁾ G.D. Hallewell,⁽²⁷⁾ E.L. Hart,⁽²⁸⁾ J.L. Harton,⁽⁸⁾ A. Hasan,⁽⁴⁾
 Y. Hasegawa,⁽²⁹⁾ K. Hasuko,⁽²⁹⁾ S. J. Hedges,⁽³⁾ S.S. Hertzbach,⁽¹⁶⁾

M.D. Hildreth,⁽²⁷⁾ J. Huber,⁽²⁰⁾ M.E. Huffer,⁽²⁷⁾ E.W. Hughes,⁽²⁷⁾ H. Hwang,⁽²⁰⁾
 Y. Iwasaki,⁽²⁹⁾ D.J. Jackson,⁽²⁵⁾ P. Jacques,⁽²⁴⁾ J. A. Jaros,⁽²⁷⁾ A.S. Johnson,⁽³⁾
 J.R. Johnson,⁽³²⁾ R.A. Johnson,⁽⁷⁾ T. Junk,⁽²⁷⁾ R. Kajikawa,⁽¹⁹⁾ M. Kalelkar,⁽²⁴⁾
 H. J. Kang,⁽²⁶⁾ I. Karliner,⁽¹³⁾ H. Kawahara,⁽²⁷⁾ H.W. Kendall,⁽¹⁵⁾ Y. D. Kim,⁽²⁶⁾
 M.E. King,⁽²⁷⁾ R. King,⁽²⁷⁾ R.R. Kofler,⁽¹⁶⁾ N.M. Krishna,⁽⁹⁾ R.S. Kroeger,⁽¹⁷⁾
 J.F. Labs,⁽²⁷⁾ M. Langston,⁽²⁰⁾ A. Lath,⁽¹⁵⁾ J.A. Lauber,⁽⁹⁾ D.W.G.S. Leith,⁽²⁷⁾
 V. Lia,⁽¹⁵⁾ M.X. Liu,⁽³³⁾ X. Liu,⁽⁶⁾ M. Loretta,⁽²¹⁾ A. Lu,⁽⁵⁾ H.L. Lynch,⁽²⁷⁾ J. Ma,⁽³¹⁾
 G. Mancinelli,⁽²²⁾ S. Manly,⁽³³⁾ G. Mantovani,⁽²²⁾ T.W. Markiewicz,⁽²⁷⁾
 T. Maruyama,⁽²⁷⁾ H. Masuda,⁽²⁷⁾ E. Mazzucato,⁽¹¹⁾ A.K. McKemey,⁽⁴⁾
 B.T. Meadows,⁽⁷⁾ R. Messner,⁽²⁷⁾ P.M. Mockett,⁽³¹⁾ K.C. Moffeit,⁽²⁷⁾
 T.B. Moore,⁽³³⁾ D. Muller,⁽²⁷⁾ T. Nagamine,⁽²⁷⁾ S. Narita,⁽²⁹⁾ U. Nauenberg,⁽⁹⁾
 H. Neal,⁽²⁷⁾ M. Nussbaum,⁽⁷⁾ Y. Ohnishi,⁽¹⁹⁾ L.S. Osborne,⁽¹⁵⁾ R.S. Panvini,⁽³⁰⁾
 H. Park,⁽²⁰⁾ T.J. Pavel,⁽²⁷⁾ I. Peruzzi,⁽¹²⁾⁽⁶⁾ M. Piccolo,⁽¹²⁾ L. Piemontese,⁽¹¹⁾
 E. Pieroni,⁽²³⁾ K.T. Pitts,⁽²⁰⁾ R.J. Plano,⁽²⁴⁾ R. Prepost,⁽³²⁾ C.Y. Prescott,⁽²⁷⁾
 G.D. Punkar,⁽²⁷⁾ J. Quigley,⁽¹⁵⁾ B.N. Ratcliff,⁽²⁷⁾ T.W. Reeves,⁽³⁰⁾ J. Reidy,⁽¹⁷⁾
 P.E. Rensing,⁽²⁷⁾ L.S. Rochester,⁽²⁷⁾ P.C. Rowson,⁽¹⁰⁾ J.J. Russell,⁽²⁷⁾
 O.H. Saxton,⁽²⁷⁾ T. Schalk,⁽⁶⁾ R.H. Schindler,⁽²⁷⁾ B.A. Schumm,⁽¹⁴⁾ S. Sen,⁽³³⁾
 V.V. Serbo,⁽³²⁾ M.H. Shaevitz,⁽¹⁰⁾ J.T. Shank,⁽³⁾ G. Shapiro,⁽¹⁴⁾ D.J. Sherden,⁽²⁷⁾
 K.D. Shmakov,⁽²⁸⁾ C. Simopoulos,⁽²⁷⁾ N.B. Sinev,⁽²⁰⁾ S.R. Smith,⁽²⁷⁾ M.B. Smy,⁽⁸⁾
 J.A. Snyder,⁽³³⁾ P. Stamer,⁽²⁴⁾ H. Steiner,⁽¹⁴⁾ R. Steiner,⁽¹⁾ M.G. Strauss,⁽¹⁶⁾
 D. Su,⁽²⁷⁾ F. Suekane,⁽²⁹⁾ A. Sugiyama,⁽¹⁹⁾ S. Suzuki,⁽¹⁹⁾ M. Swartz,⁽²⁷⁾
 A. Szumilo,⁽³¹⁾ T. Takahashi,⁽²⁷⁾ F.E. Taylor,⁽¹⁵⁾ E. Torrence,⁽¹⁵⁾ A.I. Trandafir,⁽¹⁶⁾
 J.D. Turk,⁽³³⁾ T. Usher,⁽²⁷⁾ J. Va'vra,⁽²⁷⁾ C. Vannini,⁽²³⁾ E. Vella,⁽²⁷⁾
 J.P. Venuti,⁽³⁰⁾ R. Verdier,⁽¹⁵⁾ P.G. Verdini,⁽²³⁾ S.R. Wagner,⁽²⁷⁾ A.P. Waite,⁽²⁷⁾
 S.J. Watts,⁽⁴⁾ A.W. Weidemann,⁽²⁸⁾ E.R. Weiss,⁽³¹⁾ J.S. Whitaker,⁽³⁾
 S.L. White,⁽²⁸⁾ F.J. Wickens,⁽²⁵⁾ D.A. Williams,⁽⁶⁾ D.C. Williams,⁽¹⁵⁾
 S.H. Williams,⁽²⁷⁾ S. Willocq,⁽³³⁾ R.J. Wilson,⁽⁸⁾ W.J. Wisniewski,⁽²⁷⁾
 M. Woods,⁽²⁷⁾ G.B. Word,⁽²⁴⁾ J. Wyss,⁽²¹⁾ R.K. Yamamoto,⁽¹⁵⁾ J.M. Yamartino,⁽¹⁵⁾
 X. Yang,⁽²⁰⁾ S.J. Yellin,⁽⁵⁾ C.C. Young,⁽²⁷⁾ H. Yuta,⁽²⁹⁾ G. Zapalac,⁽³²⁾
 R.W. Zdarko,⁽²⁷⁾ C. Zeitlin,⁽²⁰⁾ and J. Zhou,⁽²⁰⁾

(1) *Adelphi University, Garden City, New York 11590*

(2) *INFN Sezione di Bologna, I-40126 Bologna, Italy*

(3) *Boston University, Boston, Massachusetts 02215*

(4) *Brunel University, Uxbridge, Middlesex UB8 3PH, United Kingdom*

(5) *University of California at Santa Barbara, Santa Barbara, California 93106*

(6) *University of California at Santa Cruz, Santa Cruz, California 95064*

(7) *University of Cincinnati, Cincinnati, Ohio 45221*

(8) *Colorado State University, Fort Collins, Colorado 80523*

(9) *University of Colorado, Boulder, Colorado 80309*

(10) *Columbia University, New York, New York 10027*

(11) *INFN Sezione di Ferrara and Università di Ferrara, I-44100 Ferrara, Italy*

(12) *INFN Lab. Nazionali di Frascati, I-00044 Frascati, Italy*

- (13) *University of Illinois, Urbana, Illinois 61801*
- (14) *Lawrence Berkeley Laboratory, University of California, Berkeley, California 94720*
- (15) *Massachusetts Institute of Technology, Cambridge, Massachusetts 02139*
- (16) *University of Massachusetts, Amherst, Massachusetts 01003*
- (17) *University of Mississippi, University, Mississippi 38677*
- (19) *Nagoya University, Chikusa-ku, Nagoya 464 Japan*
- (20) *University of Oregon, Eugene, Oregon 97403*
- (21) *INFN Sezione di Padova and Università di Padova, I-35100 Padova, Italy*
- (22) *INFN Sezione di Perugia and Università di Perugia, I-06100 Perugia, Italy*
- (23) *INFN Sezione di Pisa and Università di Pisa, I-56100 Pisa, Italy*
- (24) *Rutgers University, Piscataway, New Jersey 08855*
- (25) *Rutherford Appleton Laboratory, Chilton, Didcot, Oxon OX11 0QX United Kingdom*
- (26) *Sogang University, Seoul, Korea*
- (27) *Stanford Linear Accelerator Center, Stanford University, Stanford, California 94309*
- (28) *University of Tennessee, Knoxville, Tennessee 37996*
- (29) *Tohoku University, Sendai 980 Japan*
- (30) *Vanderbilt University, Nashville, Tennessee 37235*
- (31) *University of Washington, Seattle, Washington 98195*
- (32) *University of Wisconsin, Madison, Wisconsin 53706*
- (33) *Yale University, New Haven, Connecticut 06511*
- † *Deceased*
- (a) *Also at the Università di Genova*
- (b) *Also at the Università di Perugia*

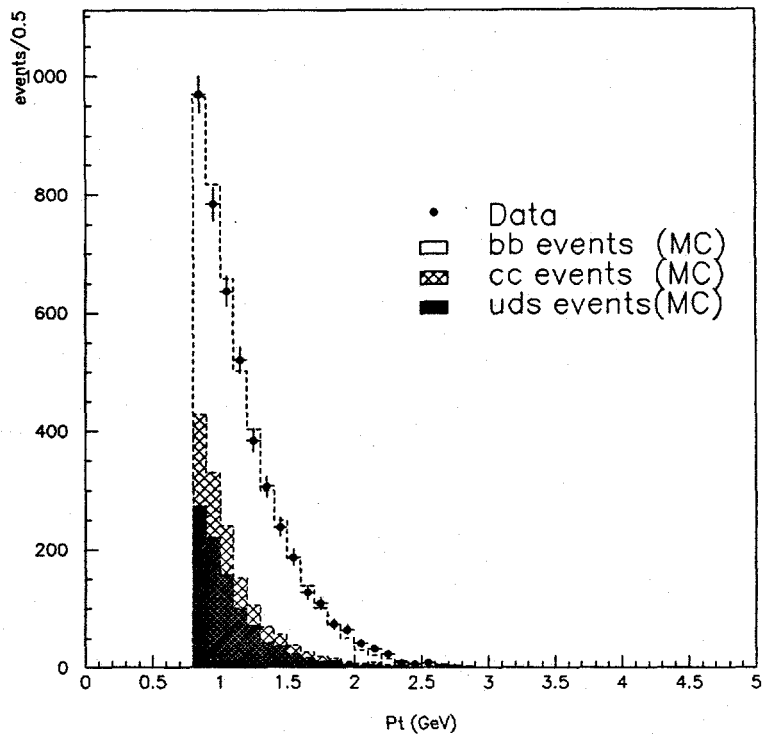


Figure 1: Distribution of momentum transverse to jet axis for selected leptons for data (points) and Monte Carlo (solid).

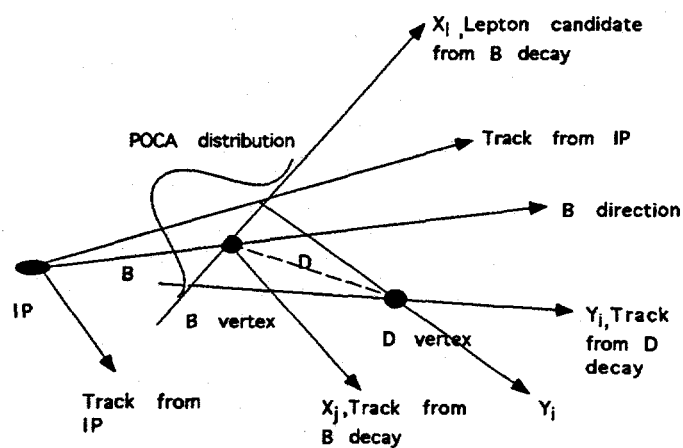


Figure 2: Illustration of the method used for B hadron decay length determination in this analysis.

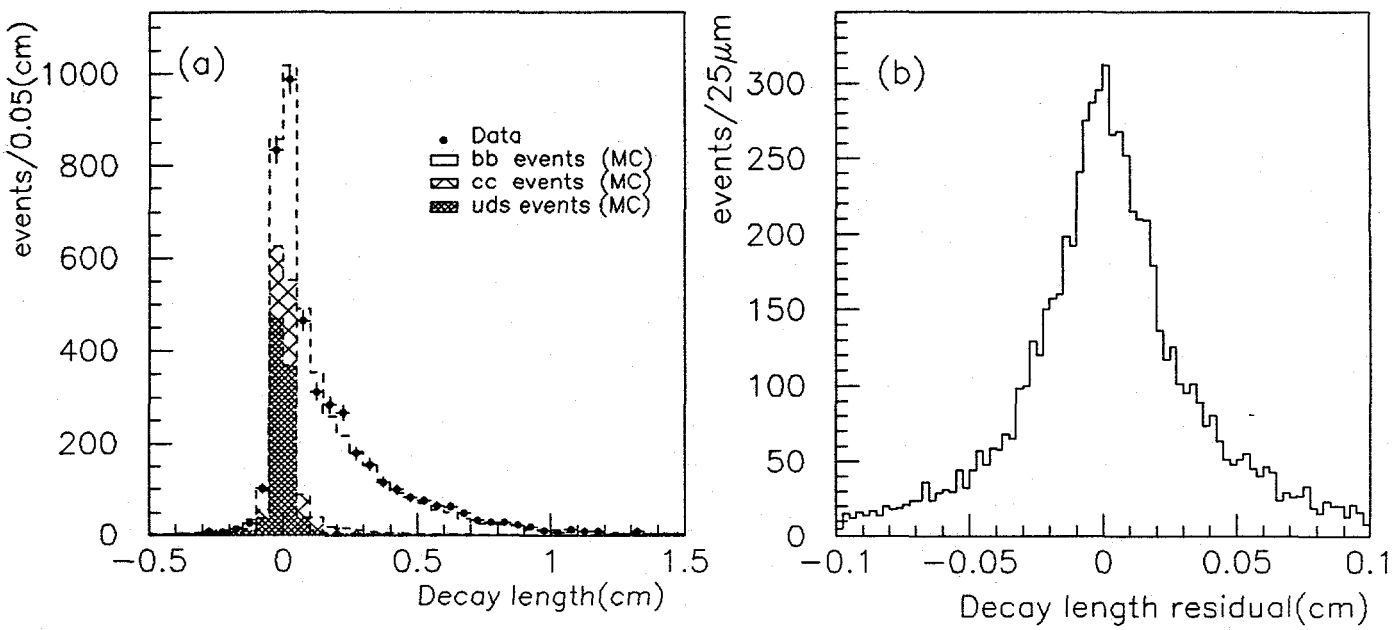


Figure 3: Reconstructed B hadron decay length (a) and decay length residual (b) for data (points) and Monte Carlo (solid).

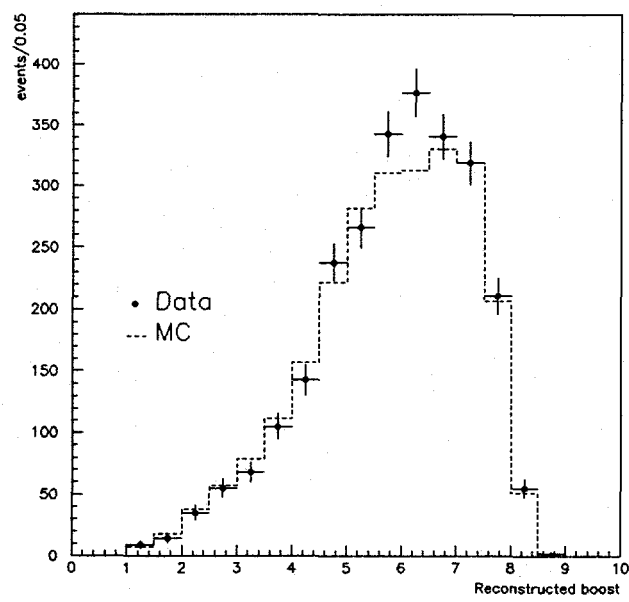


Figure 4: Reconstructed B hadron boost distribution for data (points) and Monte Carlo (solid).

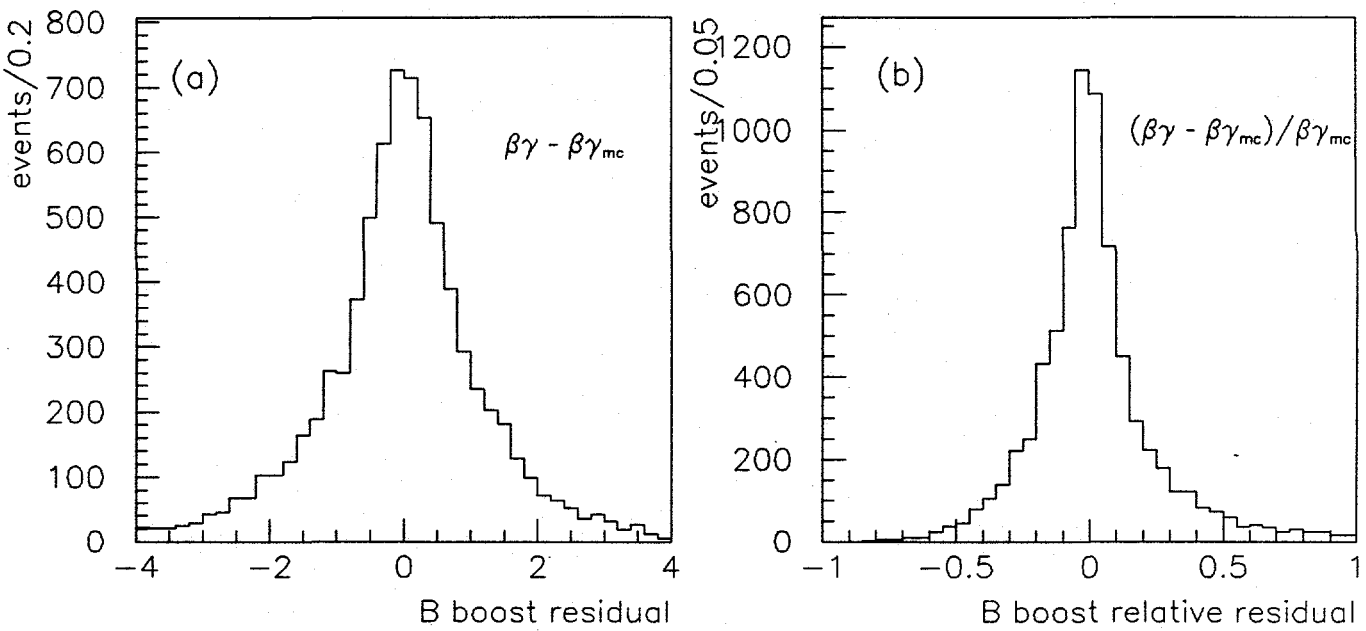


Figure 5: Boost residual (a) and relative boost residual (b) for reconstructed Monte Carlo events.

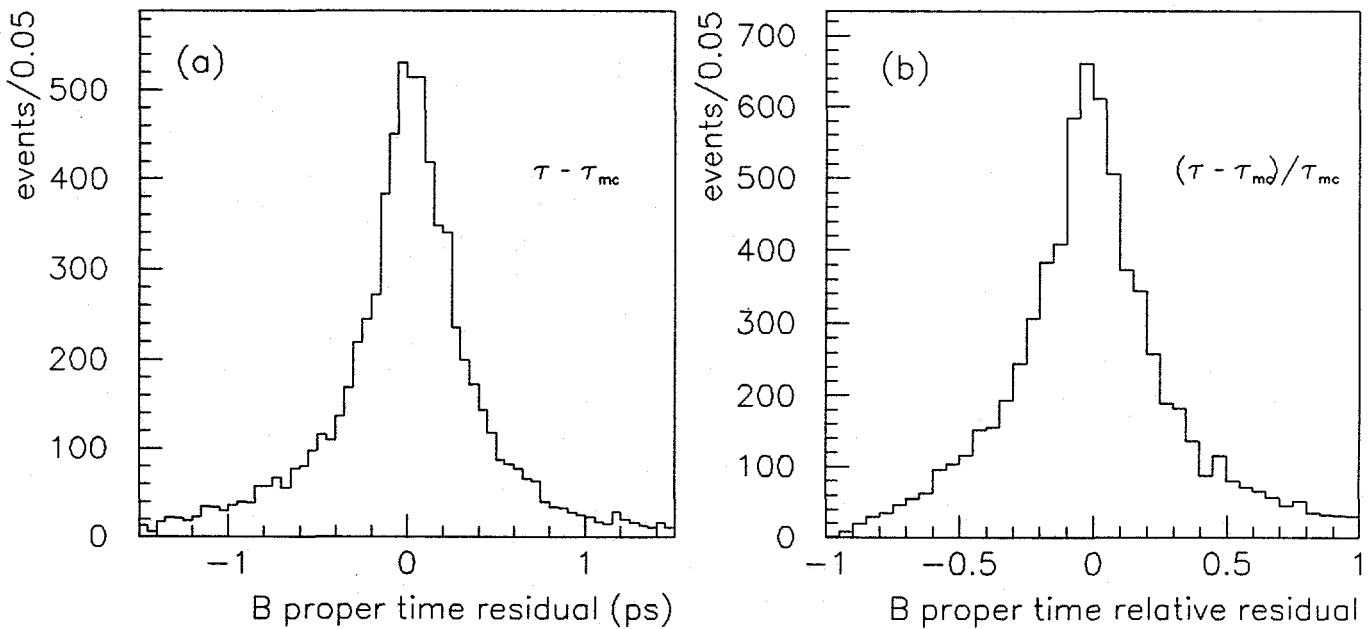


Figure 6: Proper time residual (a) and relative residual (b) for reconstructed Monte Carlo events.

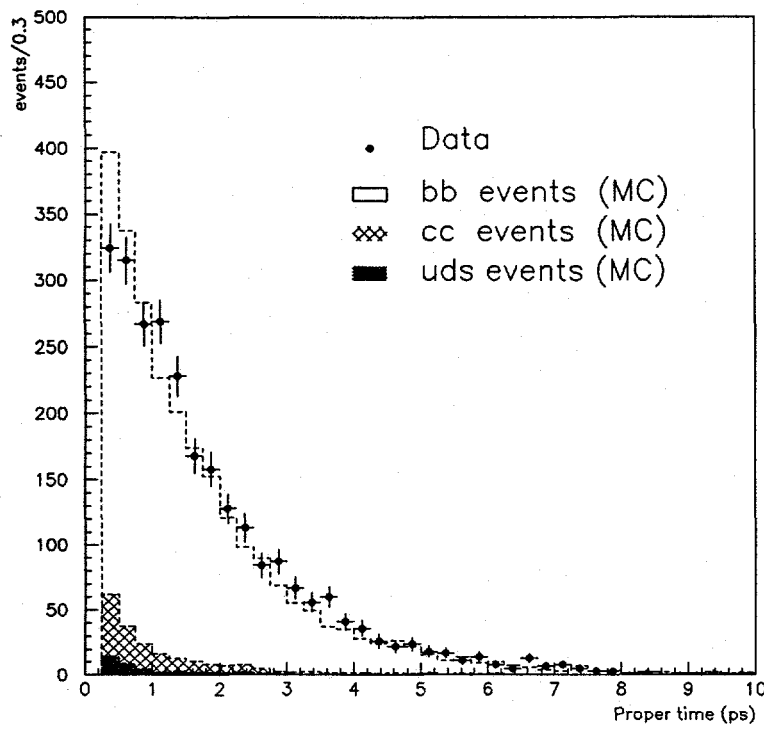


Figure 7: Proper time distribution for data (points) and reconstructed Monte Carlo events (solid).

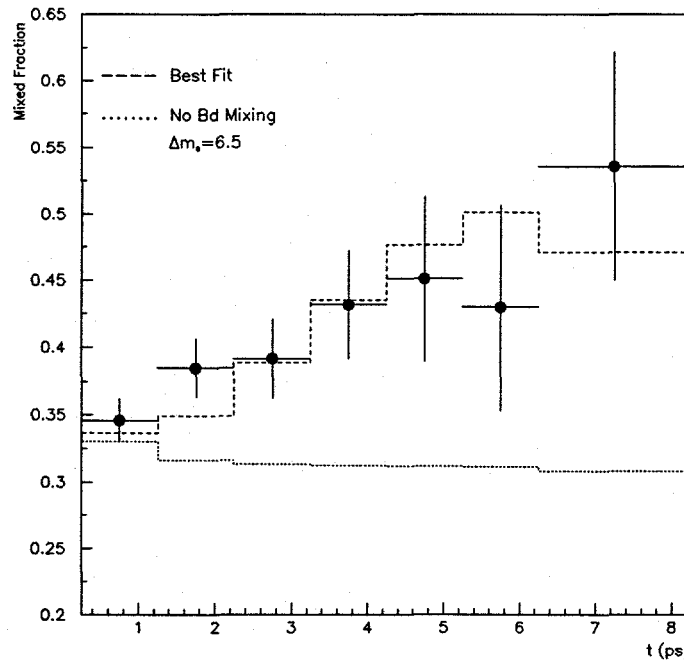


Figure 8: Mixed fraction as a function of proper time for data (points) and the best fit curve assuming $B_d^0 - \bar{B}_d^0$ mixing (solid) as well a curve representing the case with no B_d^0 mixing (dashed). For the dashed curve, B_s^0 mixing was assumed with $X_s=10$.

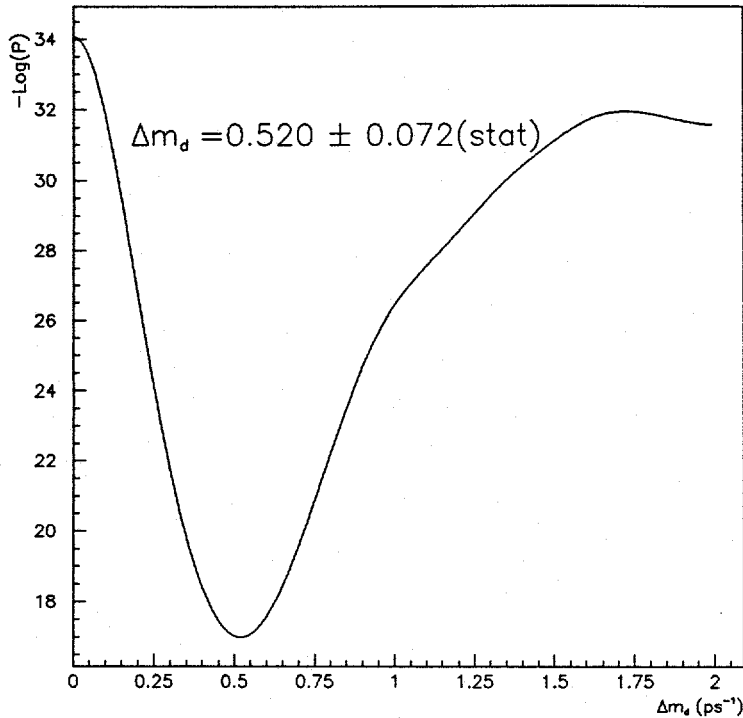


Figure 9: Log likelihood as a function of Δm_d for data.

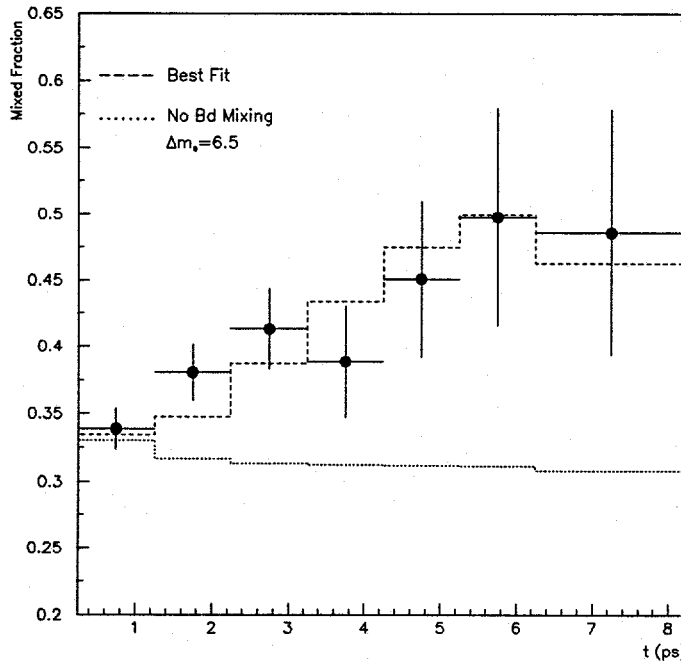


Figure 10: Mixed fraction as a function of proper time for Monte Carlo events (points) and the best fit curve assuming $B_d^0 - \bar{B}_d^0$ mixing (solid) as well a curve representing the case with no B_d^0 mixing (dashed). For the dashed curve, B_s^0 mixing was assumed with $X_s=10$.

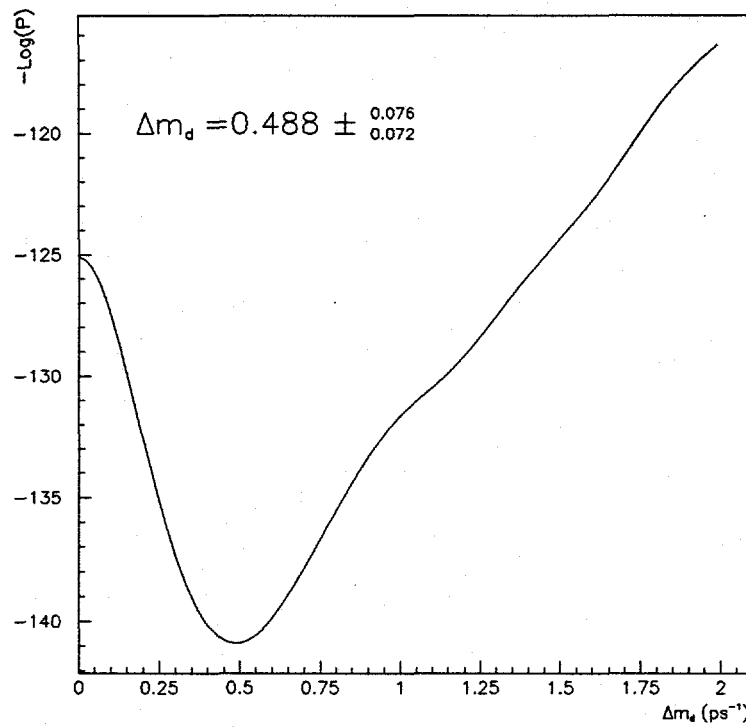


Figure 11: Log likelihood as a function of X_d for Monte Carlo events.